Robust Projected Weakening of Winter Monsoon Winds Over the Arabian Sea Under Climate Change

Vallivattathillam Parvathi, Iyyappan Suresh, Matthieu Lengaigne, Takeshi Izumo, Jérôme Vialard

AGU PUBLICATIONS

Geophysical Research Letters

RESEARCH LETTER
10.1002/2017GL075098

Key Points:
- This study reports a robust reduction of the northeast monsoon winds over the Arabian Sea under two climate change scenarios
- The wind weakening is driven by a reduction of the Interhemispheric sea level pressure gradient
- Weakening of winds leads to a reduced winter mixed layer deepening in the northern Arabian Sea and hence less oceanic productivity

Supporting Information:
- Supporting Information S1

Correspondence to:
I. Suresh,
isuresh@nio.org

Citation:
Parvathi, V., Suresh, I., Lengaigne, M., Izumo, T., & Vialard, J. (2017). Robust projected weakening of winter monsoon winds over the Arabian Sea under climate change. *Geophysical Research Letters*, *44*, 9833–9843. https://doi.org/10.1002/2017GL075098

Received 26 JUL 2017
Accepted 9 SEP 2017
Accepted article online 14 SEP 2017
Published online 4 OCT 2017

Robust Projected Weakening of Winter Monsoon Winds Over the Arabian Sea Under Climate Change

V. Parvathi[1], I. Suresh[1], M. Lengaigne[2,3], T. Izumo[2,3], and J. Vialard[2]

[1]CSIR-National Institute of Oceanography, Panaji, India, [2]Sorbonne Universités (UPMC, Univ Paris 06)-CNRS-IRD-MNHN, LOCEAN Laboratory, IPSL, Paris, France, [3]Indo-French Cell for Water Sciences, IISc-NIO-IITM–IRD Joint International Laboratory, NIO, Panaji, India

Abstract The response of the Indian winter monsoon to climate change has received considerably less attention than that of the summer monsoon. We show here that all Coupled Model Intercomparison Project Phase 5 (CMIP5) models display a consistent reduction (of 6.5% for Representative Concentration Pathways 8.5 and 3.5% for 4.5, on an average) of the winter monsoon winds over the Arabian Sea at the end of 21st century. This projected reduction weakens but remains robust when corrected for overestimated winter Arabian Sea winds in CMIP5. This weakening is driven by a reduction in the interhemispheric sea level pressure gradient resulting from enhanced warming of the dry Arabian Peninsula relative to the southern Indian Ocean. The wind weakening reduces winter oceanic heat losses to the atmosphere and deepening of convective mixed layer in the northern Arabian Sea and hence can potentially inhibit the seasonal chlorophyll bloom that contributes substantially to the Arabian Sea annual productivity.

Plain Language Summary The Indian summer monsoon response to climate change has been previously the focus of many studies. The Indian winter monsoon-projected response to climate change is, however, largely unexplored. This is the first study to report a robust weakening of the Indian winter monsoon winds over the Arabian Sea in two Coupled Model Intercomparison Project Phase 5 scenarios (an unmitigated and a mitigated one). The wind weakening leads to reduced winter oceanic convective overturning in the northern Arabian Sea. This winter convection is the key mechanism for a productivity (winter) bloom that strongly contributes to the Arabian Sea annual productivity. The projected winter monsoon weakening may thus reduce the Arabian Sea productivity. We also show a rainfall increase that could affect water supply in tropical Indian Ocean islands and Eastern Africa.

1. Introduction

The Indian subcontinent experiences the most energetic and vigorous monsoon system globally (Gadgil, 2003; Webster et al., 1998). During boreal summer, the Asian continent warms faster than the Indian Ocean (IO), favoring the northward movement of the Intertropical Convergence Zone (Trenberth et al., 2000) and the development of a low-level cross-equatorial jet (Findlater, 1971; Figure S1a in the supporting information). The associated southwesterly winds transport moisture collected over the southern IO and the Arabian Sea (AS) toward the Indian subcontinent, giving rise to the Indian Summer Monsoon (ISM) rainfall. As the livelihood of this densely populated region critically depends on this water supply (Gadgil & Gadgil, 2006), a large body of literature has already investigated the influence of anthropogenic climate change on the ISM (e.g., Goswami et al., 2006; Roxy et al., 2015; Turner & Annamalai, 2012). Comparisons of present and future simulations from the Coupled Model Intercomparison Project Phase 5 (CMIP5) indicate a consistent increase of future ISM rainfall (e.g., Endo & Kitoh, 2016; Ogata et al., 2014; Sharmila et al., 2015; Sooraj et al., 2015), as well as a general weakening of the large-scale ISM circulation (Sooraj et al., 2015) and poleward shift of the AS low-level jet (Sandeep & Ajayamohan, 2015; Figures S1b–S1d).

During boreal winter, the Eurasian continent cools while the southern tropical IO warms. The resulting high pressure over the Arabian Peninsula and low pressure under the Intertropical Convergence Zone (ITCZ) around 10°S drive the Indian Winter Monsoon (IWM), characterized by northeasterly winds over the AS (Figure 1a). While IWM contributes significantly to the annual precipitation over the Himalayan region (e.g., Dimri et al., 2015) and the southeastern India and Sri Lanka (e.g., Rajeevan et al., 2012; Vialard et al., 2011), most of the rainfall occurs over the ocean around 10°S, thereby forming only a small fraction of the annual rainfall over India. Nonetheless, the winter monsoon has its most important implications for the

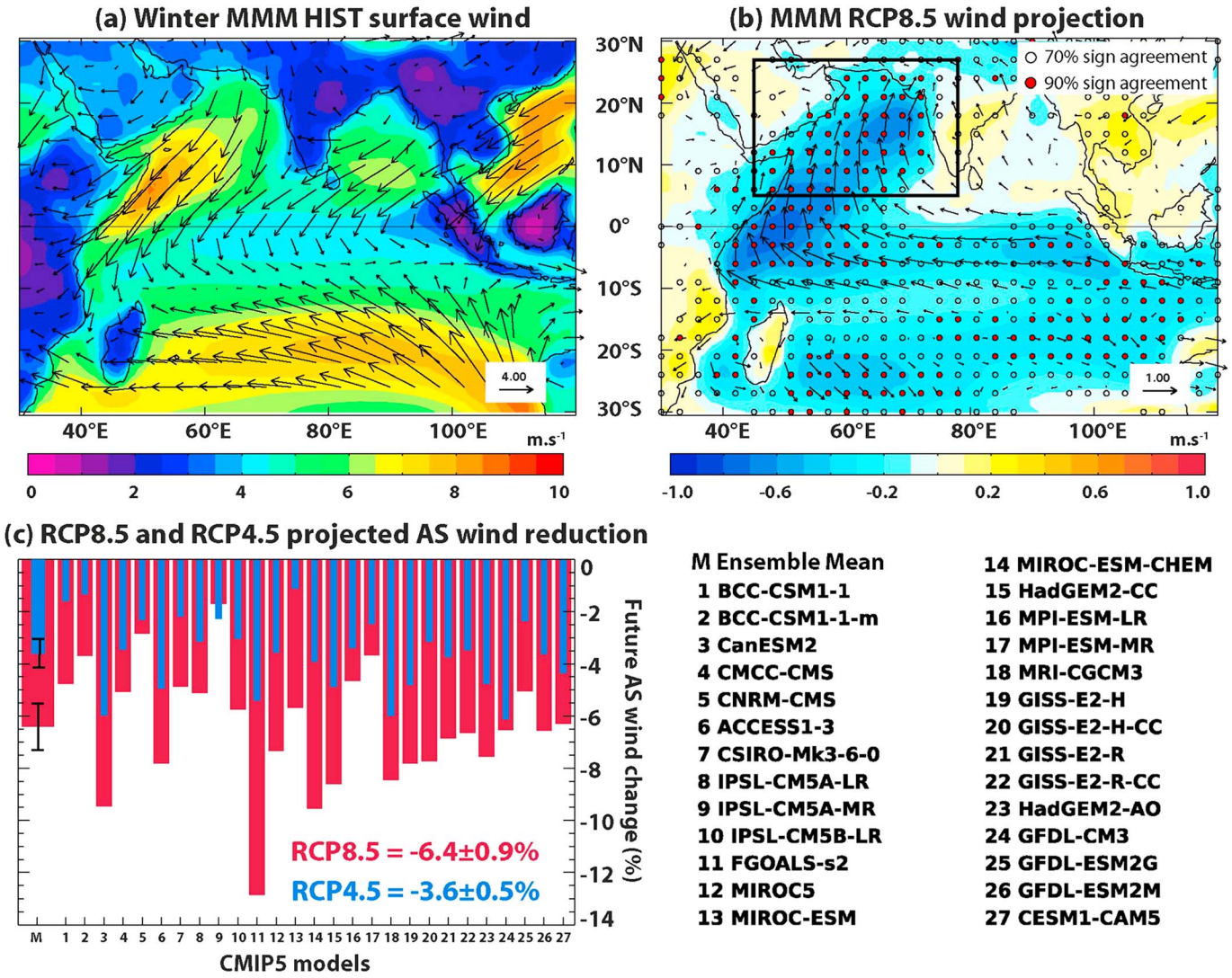

Figure 1. Multimodel mean (MMM) winter (DJFM) climatology of surface winds (vectors) and speed (color) for (a) present climate (HIST) and (b) RCP8.5 projected changes. Regions where more than 70% (90%) models agree on the sign of the wind speed change are indicated with black circle (red dots) in Figure 1b. (c) Bar plot of the percentage of projected surface wind speed changes in RCP8.5 (red) and RCP4.5 (blue) scenarios in winter within the AS (black frame in Figure 1b for individual models and MMM with black whiskers indicating the 95% confidence interval (values indicated) on the mean. The models used in the present study (with model IDs) are listed in the bottom right panel.

biogeochemistry and ecosystems of the northern IO (e.g., Smith & Madhupratap, 2005). The evaporative cooling associated with the cold and dry IWM winds induces convective overturning in the northern AS, contributing to the ventilation of the nearly anoxic subsurface waters (Morrison et al., 1999). The convective overturning also entrains nutrients into the surface euphotic layer (Keerthi et al., 2017; Prasanna Kumar et al., 2001), leading to a prominent chlorophyll bloom (e.g., Banse & McClain, 1986). This bloom contributes substantially to the total annual AS primary productivity (Madhupratap et al., 1996; Marra & Barber, 2005) and occurs when the winter oceanic conditions are more favorable for fishing activities than the summer leading to the highest fish catch (Madhupratap et al., 2001).

There is to date no study focusing on the projected IWM response to the global warming. Given its importance for the AS climate and biogeochemistry, the present study aims at assessing the influence of global warming on the IWM by analyzing the present-day and the future simulations from CMIP5 models. This paper is organized as follows. Section 2 introduces the data and methods. Section 3 shows that there is a weakening of IWM winds over the Arabian Sea in CMIP5 models, under both RCP8.5 and 4.5 scenarios, even when model bias is accounted for. Furthermore, this section discusses the impacts and the possible underlying

mechanisms of this monsoon weakening. Finally, section 4 summarizes the results and discusses their limitations and implications.

2. Data and Methodology

2.1. Data

In this study, we compare the historical simulations (HIST) forced by the observed anthropogenic and natural forcing with the future simulations performed under two contrasted Representative Concentration Pathways (RCP) scenarios: RCP8.5, an unmitigated scenario with radiative forcing reaching 8.5 W m^{-2} by 2100, and RCP4.5, a mitigated scenario with radiative forcing reaching 4.5 W m^{-2} by 2100 (Moss et al., 2010). We analyze monthly mean outputs from 27 CMIP5 models for which 10 m surface winds are available for historical, RCP8.5 and RCP4.5 simulations. When several ensemble members are available, we choose only the first one, in order to assign the same weight to all models. When available, we analyze the monthly precipitation, surface skin temperature (Tsurf), mean sea level pressure (SLP), wind stress, net surface heat flux (HFlx), and mixed layer depth (MLD) from these models. Details on the available variables for each model are provided in Table S1.

The biases in historical simulations are computed over the 1986–2005 period relative to Tropflux (Praveen Kumar et al., 2012) for surface winds at 10 m, surface temperature, and air-sea fluxes; ERA-Interim (Dee et al., 2011) for SLP; and de Boyer Montégut et al. (2004) climatology for MLD.

2.2. Methodology

The seasonal average for winter monsoon is defined as the December–March (DJFM) average and that for summer monsoon as the June–September average. In order to allow a fair comparison, all data sets are regridded to a common 1° × 1° horizontal grid. We define the present-day climatology of individual models as the 20 year (1986–2005) mean of historical simulations, the future climate as the 20 year (2080–2099) mean of RCP8.5 and RCP4.5 simulations, and the projected climate change as their difference (i.e., RCP minus HIST). We show the Multimodel mean (MMM) of either the projected response to climate change or bias in order to highlight the consensus across models. As in previous studies (e.g., Christensen et al., 2013), medium (high) robustness is defined when at least 70% (90%) of models agree on the sign of the projected change or bias.

3. Results

3.1. Robust Weakening of the Winter Monsoon Circulation

Figure 1b illustrates that the projected RCP8.5 MMM winter surface winds weaken over most of the IO, except in the Bay of Bengal. This widespread weakening is robust in more than 70% of models over most of the IO (black circles on Figure 1b), with the largest and most coherent changes over the AS and western equatorial IO, where more than 90% of the models agree (red dots on Figure 1b). Red bars on Figure 1c further detail the percentage of AS average wind speed reduction relative to the present climate average for each model in the RCP8.5 scenario. Every model (out of the 27 for which surface winds are available) projects a weakening of winter winds over the AS by the end of the 21st century, ranging from 2 to 13%. The projected RCP8.5 MMM AS wind reduction is 6.4 ± 0.9%, at the 95% confidence level. Blue bars on Figure 1c illustrate that this wind reduction, although weaker, is also very robust when considering the more optimistic RCP4.5 scenario. In this case, the AS wind reduction ranges from 2 to 6%, with MMM reduction of 3.6 ± 0.5% at 95% level.

This consistent weakening of the IWM circulation in future CMIP5 simulations may, however, result as an artifact of the present-day model biases in the IO. Li, Xie, and Du (2016), for instance, showed that most CMIP5 models overestimate the present-day amplitude of the IO dipole (IOD), the main intrinsic mode of interannual SST variations in the IO (e.g., Saji et al., 1999). They further suggest that this overestimation largely explains the consistent IOD-like warming response to climate change in most CMIP5 models, with a stronger IOD-like warming pattern in models with higher IOD amplitude. There is, however, no relation between the projected AS wind weakening and the IOD amplitude in CMIP5 models (r = 0.15, not significant at the 90% level; not shown). On the other hand, CMIP models display other biases, which may influence the projected IWM response to climate change. For instance, most CMIP models tend to display a strong IWM, leading to a

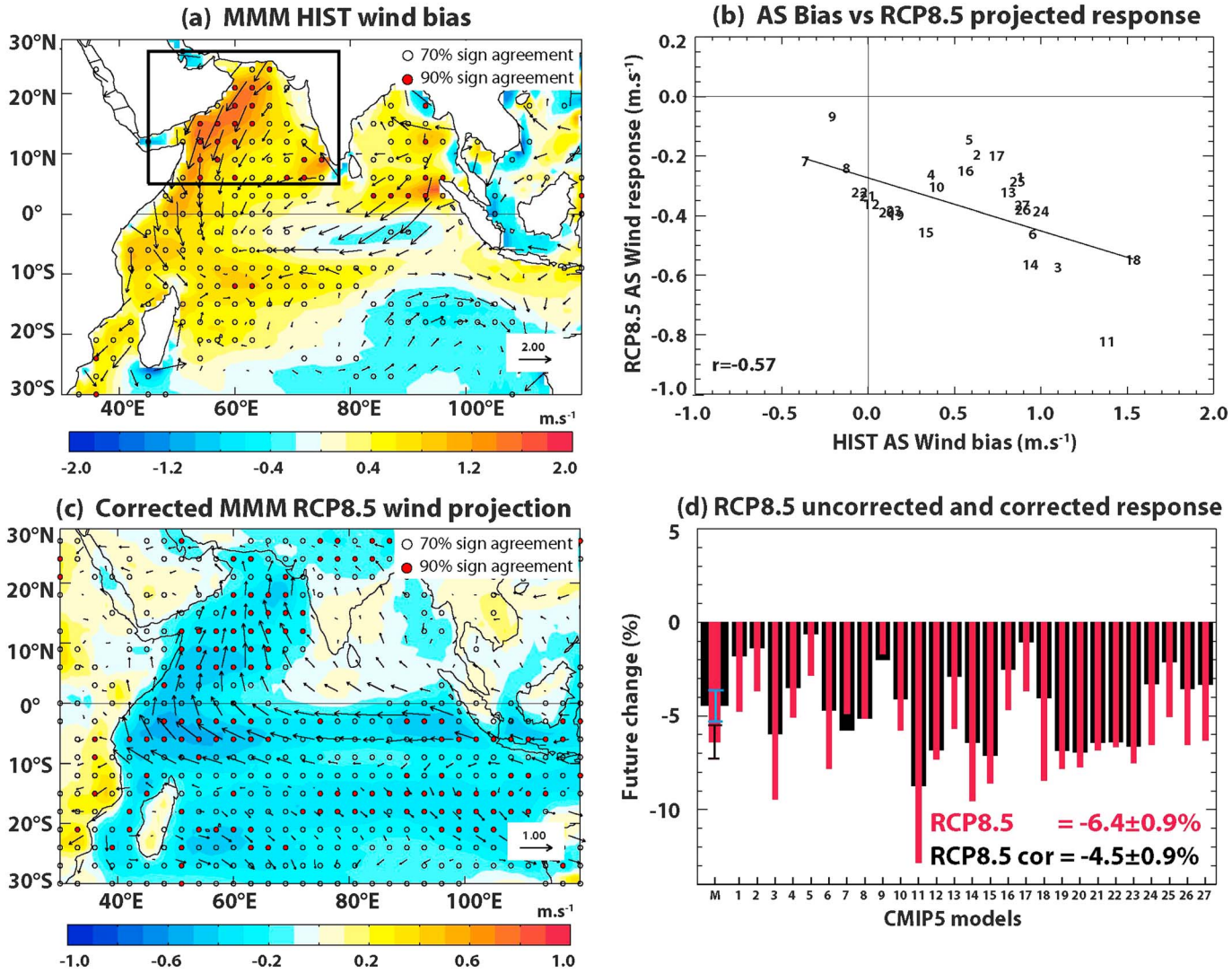

Figure 2. (a) Multimodel mean (MMM) bias in the winter wind speed climatology relative to the Tropflux data set. (b) Scatterplot of average AS winter wind speed bias versus RCP8.5 wind speed projected change for individual models (see Figure 1 for model IDs). The regression line and correlation value are also shown. (c) MMM RCP8.5 projected winter bias corrected (see text and supporting information for details) wind speed changes. (d) Bar plot of the percentage of future RCP8.5 surface wind speed corrected (black) and uncorrected (red) changes in the AS (black frame on Figure 2a for individual models and MMM with whiskers indicating the 95% confidence interval (values indicated) on the mean. Regions where more than 70% (90%) models agree on the sign of the wind speed bias/changes are indicated with black circle (red dots) on Figures 2a/2c.

cold SST bias over the AS (Sperber et al., 2013), which has received some attention because it leads to unrealistic rainfall in the following summer monsoon by reducing the evaporation over the AS (Levine et al., 2013; Marathayil et al., 2013; Sandeep & Ajayamohan, 2014).

Figure 2a illustrates this strong IWM winds bias in the CMIP5 MMM, with an overestimated cross-equatorial jet over the western IO and IWM circulation over the AS. The present-day AS wind speeds are on an average overestimated by ~0.6 m s^{-1} (~9%). The amplitude and sign of this bias, however, varies considerably among models (Figure 2b), ranging from a weak underestimation of −0.4 m s^{-1} to a strong overestimation of 1.5 m s^{-1}. The amplitude of the AS winter wind reduction in the RCP8.5 scenario is related to the amplitude of the IWM wind bias ($r = -0.57$ significant at 99% level): models with larger IWM climatological winds (and thus larger bias) generally predict a larger reduction of IWM circulation (Figure 2b). We can hence adopt a strategy similar to that of Li, Xie, and Du (2016) and use the statistical linear relation between the model bias and the projected response to climate change to extrapolate the response to that at zero bias (computational details provided in the supporting information). This statistical strategy, known as "emergent constraints,"

has already been widely used to provide reliable future projections (e.g., Bracegirdle & Stephenson, 2012, 2013; Cox et al., 2013; Li, Xie, Du, & Luo 2016).

The resulting corrected RCP8.5 surface wind changes are displayed in Figure 2c. The RPC8.5 MMM winter winds over the AS exhibit weakening even when accounting for the present-day IWM biases. The amplitudes of the uncorrected and corrected RCP8.5 projected AS wind speed changes are provided in Figure 2d. Although reduced when applying the bias correction, there is still a robust IWM circulation reduction in response to climate change in all models (Figure 2d; MMM AS wind reduction with correction is 4.5 ± 0.9% at the 95% confidence level against 6.4 ± 0.9% without correction). The projected weakening is also robust when applying the bias correction to RCP4.5 projections (2.5 ± 0.5%, Figure S2). Thus, the projected IWM circulation weakening is robust in all of the analyzed CMIP5 models under different scenarios, even after accounting for the present-day model biases. Henceforth, for conciseness, we discuss only the RCP8.5 projections, though our conclusions hold true for RCP4.5 projections as well.

3.2. Impacts of the Projected IWM Weakening

As mentioned in section 1, the RCP8.5 projected summer monsoon response is associated with a consistent 20 ± 6% increase in rainfall over India (Figures S3a and S3c) (Endo & Kitoh, 2016; Ogata et al., 2014; Sharmila et al., 2015; Sooraj et al., 2015). The climate change also induces increased rainfall in the winter monsoon rainy zones in the equatorial IO (Figures S3b and S3d). This projected rainfall increase is, however, weaker (~10 ± 2%; Figures S3d versus S3c) and occurs mostly over the ocean and hence is of lesser relevance from a socioeconomic viewpoint compared to its summer counterpart, except for the east African countries and islands located in the equatorial region.

On the other hand, the IWM has important implications for the AS biogeochemistry. The cold and dry air blowing from the continent induces strong evaporative heat losses to the atmosphere in the northern AS. This combines with the mechanical stirring by the northeasterly winds to induce a mixed layer deepening, which in turn drives the winter blooms in the northern AS (Banse & McClain, 1986; Madhupratap et al., 1996; Morrison et al., 1999). Figure 3 shows the projected IWM surface HFlx and MLD responses. The surface wind weakening induces a reduction of the latent cooling, which is strongest in the northern AS, where the thermodynamical imbalance between the ocean and cold, dry IWM winds is largest (Figure 3a). All but three models exhibit a reduction of the winter surface heat losses in the northern AS (Figure 3c, 15 ± 5% at 95% confidence level for RCP8.5 MMM, 10 ± 5% when corrected for the wind bias). The surface cooling reduction is strongly correlated ($r = -0.78$, 99% level confidence; Figure S4a) with the wind reduction over the northern AS, suggesting that the wind weakening drives latent and thus net heat flux reduction.

Air-sea fluxes of momentum have a quadratic dependence on the winds and hence would reduce roughly twice as that of the wind reduction in terms of the percentage. Indeed, the projected AS wind weakening also reduces the momentum flux at the air-sea interface, leading to a consistent wind stress reduction over the AS (Figure S5), which is more than 2 times the wind reduction in percentage (−15 ± 2% at 95% confidence level for RCP8.5 MMM; Figure S5c). The reduced heat losses at the surface and the reduced mechanical stirring both favor a shallower MLD, leading to a very consistent projected MLD shoaling in the northern AS (15 ± 3% at 95% confidence level for RCP8.5 MMM; Figures 3b and 3d). As expected, the amplitude of this shoaling correlates reasonably well ($r = 0.65$) with the amplitude of the wind reduction over the northern AS (Figure S4b).

The bias correction approach described in the previous section (i.e., correcting the projected response on the basis of AS wind speed bias) when applied to the HFlx and MLD yields a very consistent reduction across all models (Figures 3c and 3d), with RCP8.5 MMM 10 ± 5% and 11 ± 2%, respectively. As for the wind speed, the HFlx and MLD are also overestimated in CMIP5 (not shown). The reduction in HFlx and MLD responses remains robust even when performing the correction on the basis of their respective biases (8 ± 5% and 13 ± 3%, respectively), which will account for the potential nonlinearities (not shown).

3.3. Mechanisms

In this section, we discuss the possible mechanisms responsible for the reduced IWM circulation in response to the anthropogenic global warming.

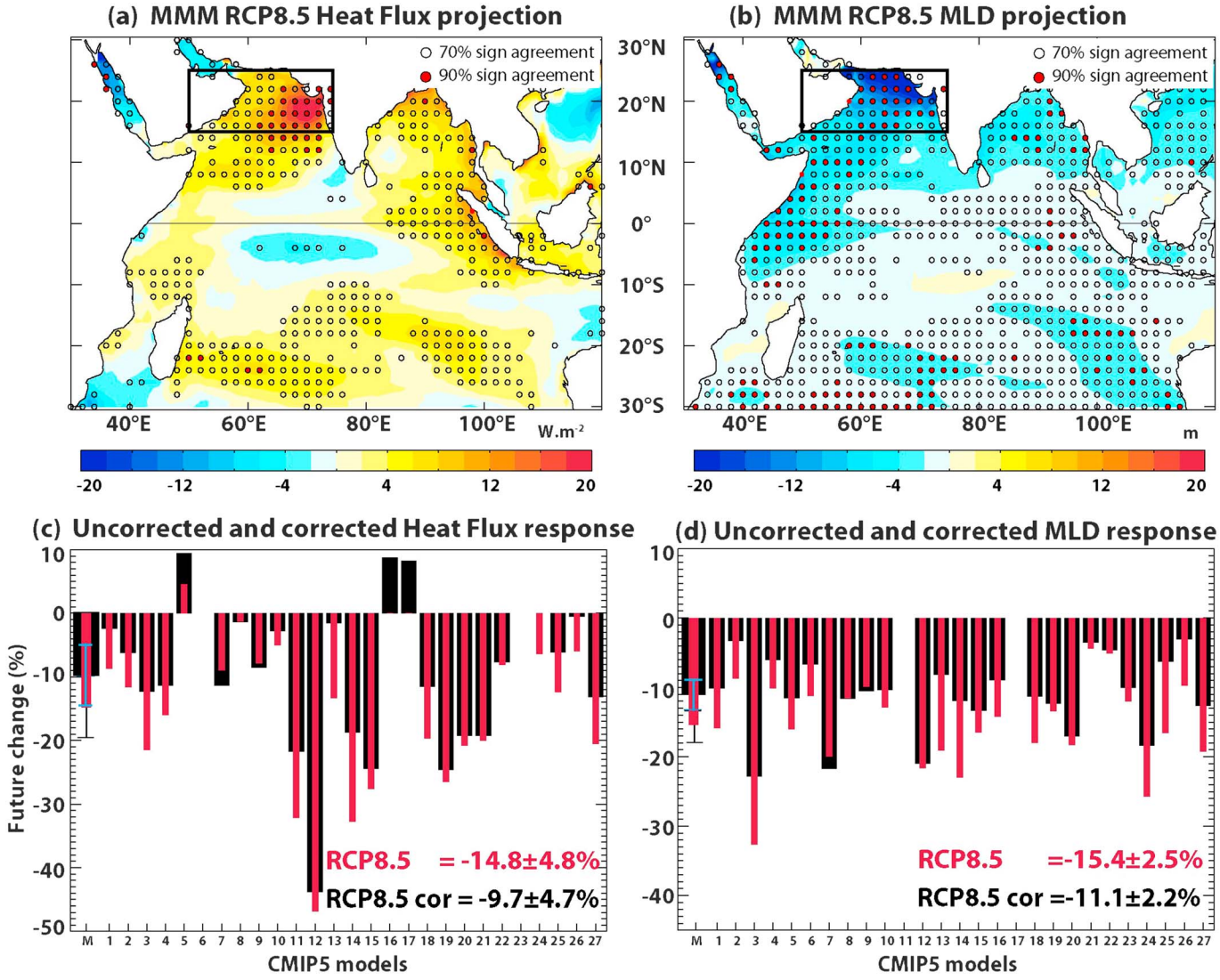

Figure 3. Multimodel mean (MMM) winter RCP8.5 (a) net heat flux (HFlx, positive downward) and (b) MLD projected changes. Regions where more than 70% (90%) models agree on the sign of the change are indicated with black circle (red dots) on Figures 3a and 3b. Bar plots of the percentage of future RCP8.5 (c) HFlx and (d) MLD corrected and uncorrected changes in the northern AS box (black frame on Figures 3a and 3b) for individual models and MMM with whiskers indicating the 95% confidence interval (values indicated) on the mean.

The winter monsoon arises from an interhemispheric SLP gradient, which constrain the surface winds through geostrophy. The IWM winds are clearly associated with a high pressure over the Arabian Peninsula and a low pressure below the ITCZ around 5–10°S (Figure S6), with frictional effects in the surface layer contributing to a veering toward low-pressure area relative to isobars in the Northern Hemisphere (e.g., chapter 9.2 in Gill, 1982). As a result, the present-day (HIST) AS wind speed has a 0.71 correlation with HIST interhemispheric SLP gradient between the Arabian Peninsula and the southern Indian Ocean (Figure 4a; see Figure S7a for a justification of the two selected boxes to calculate the interhemispheric SLP gradient). This interhemispheric SLP gradient is itself strongly correlated ($r = -0.69$) with the interhemispheric Tsurf gradient (Figures 4b and S6). Overall, in present-day climate, CMIP5 models with a larger Tsurf contrast between the cold Arabian Peninsula and warmer southern IO in winter have a stronger interhemispheric SLP gradient and stronger winter AS surface winds (Figures 4a and 4b). We now investigate these relationships in the context of projected climate change.

Figures 4c and 4d display the MMM future Tsurf and SLP changes. SLP increases over the southern IO and decreases over the Arabian Peninsula, northern AS, and western India (Figure 4d). Consequently, the

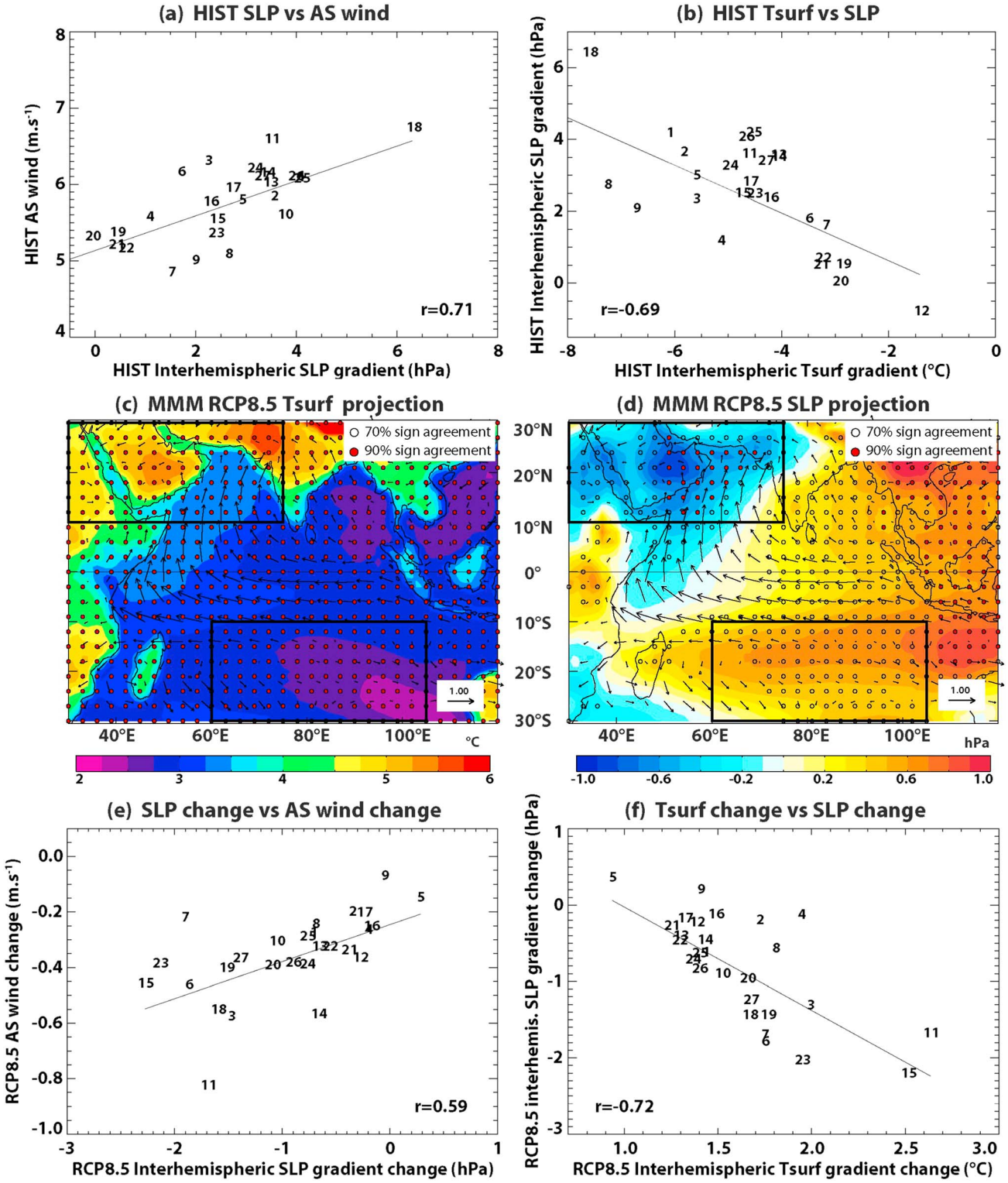

Figure 4. Scatterplots of present-day (HIST) interhemispheric sea level pressure gradient against (a) HIST AS wind speed (box shown in Figure 1b) and (b) HIST land-sea interhemispheric surface temperature (Tsurf) gradient for individual models. Interhemispheric gradients are calculated as the difference between the averaged values over boxes (north minus south) shown in Figures 4c and 4d. Multimodel mean (MMM) winter climatology of RCP8.5 projected changes for (c) Tsurf (°C) and (d) mean sea level pressure (hPa; SLP) with wind changes overlaid as vectors. Regions where more than 70% (90%) models agree on the sign of the change are indicated with black circle (red dots) on both panels. Scatterplot of RCP8.5 projected interhemispheric SLP gradient changes against (e) wind speed changes in the AS (box in Figure 1b) and (f) interhemispheric land-sea Tsurf gradient changes. See Figure 1 for model ID for each model on scatterplots. The regression lines and correlation values are also shown on Figures 4a, 4b, 4e, and 4f.

interhemispheric SLP gradient reduces, resulting in a weakening of the IWM winds. There is indeed a 0.59 cross-model correlation (significant at the 99% level) between the projected AS winter wind speed and interhemispheric SLP gradient changes (Figure 4e; Figure S7b justifies the selection of the two boxes).

This interhemispheric SLP change is related to an interhemispheric Tsurf change. Under a warming scenario, land warms much more than the ocean (Figure 4c) (Boer, 2011; Dommenget, 2009; Joshi et al., 2008). This results in a projected 1 to 2.5°C decrease of the interhemispheric Tsurf contrast in CMIP5 models (Figure 4f). The faster land warming is not related to the lower heat capacity of the land, rather to the larger lapse rate over the land, as the troposphere over the land generally is drier than that over the oceans (e.g., Joshi et al., 2008). The upper tropospheric warming is relatively uniform in the tropics (e.g., Sobel et al., 2001): a larger lapse rate hence yields a larger surface warming over land, in particular in dry areas. This explains the relatively large warming over the dry Arabian Peninsula and Thar dessert and weaker warming over the southern IO. The SLP change, in general, mirrors the Tsurf change (Figures 4c and 4d). In particular, the projected changes in interhemispheric Tsurf and SLP gradients are highly correlated ($r = -0.72$ significant at the 99% level; Figure 4f). Overall, the CMIP5 models with the larger Arabian Peninsula warming relative to the southern IO are those with the stronger interhemispheric SLP gradient and more weakening in the AS wind speed.

Although there is a relatively good agreement between SLP and Tsurf changes, they do not match perfectly (Figures 4c and 4d). Bayr and Dommenget (2013) have indeed shown that the SLP response to global warming is much more closely related to the average tropospheric (1,000 to 100 hPa) temperature than to Tsurf (because of the hydrostatic relation). There is, however, a relatively strong control of Tsurf on SLP, as illustrated by the relatively high correlation between the interhemispheric Tsurf and SLP changes (Figure 4f). Indeed, as the tropical tropospheric temperature is nearly uniform at higher levels (e.g., Bayr & Dommenget, 2013), most of the warming differences occur at lower levels. The near-surface warming is largely driven by the near-surface humidity content (e.g., Bayr & Dommenget, 2013) that exerts a strong control on the average tropospheric temperature and hence on SLP.

While our study focuses on the projected wind changes, we also briefly assess the projected rainfall changes (Figures S3b and S3d). Despite a decrease in the winter monsoon winds, the projected winter rainfall (Figures S3b and S3d) increases under the intertropical convergence zone. As noted by Held and Soden (2006), the tropospheric warming induced by climate change results in increased water vapor concentrations owing to the Clausius-Clapeyron relation and hence to enhanced moisture convergence. This effect probably overcomes that of the weaker horizontal circulation (which diminishes the moisture convergence), leading to increased rainfall. We, however, note that there are uncertainties in the projected regional rainfall in CMIP models (e.g., Hwang & Frierson, 2013; Sabeerali et al., 2015) and that these rainfall projections should hence be taken cautiously.

4. Summary and Discussion

Our results indicate a robust reduction of the IWM wind intensity in CMIP5 models (Figure 1), comparable to the wind intensity changes associated with the poleward shift of the monsoon jet in summer (Figures S1b–S1d). This IWM wind reduction is related to an enhanced warming of the Arabian Peninsula relative to the southern Indian Ocean that reduces the interhemispheric temperature and SLP gradients. Compared with its summer counterpart, a few studies have discussed the future changes of the winter monsoon in the Asian sector (see review by Kitoh, 2017), largely focusing on the East Asian region. CMIP simulations generally project a weakening (strengthening) of the East Asian winter monsoon circulation north (south) of 25°N, as a result of a northward shift of the Aleutian low and decreased northwest-southeast thermal and SLP differences across northeast Asia (e.g., Jiang & Tian, 2013). These simulations also project a rainfall increase related to the southeast Asian winter monsoon in response to cyclonic wind anomalies over the south China Sea (Siew et al., 2014). Although evident in some of the analyses dedicated to East Asian winter monsoon projections (e.g., Figure 7 from Ogata et al., 2014 and Figure 8 from Kitoh, 2017), this study is the first to discuss the projected decrease of the IWM circulation over the AS and the driving mechanisms. While both summer and winter Indian monsoonal circulation slowdown in CMIP models have been tracked back to changes in meridional temperature gradients between the IO and the northern IO landmass, the key continental regions involved differ substantially, with the summer monsoon involving temperature changes over the Tibetan

Plateau (e.g., Sooraj et al., 2015) and winter monsoon being mainly influenced by temperature and SLP changes over the Arabian Peninsula and the Thar dessert.

The projected AS weakening discussed here is stronger (-0.38 m s^{-1}/-6.5%; RCP8.5) than the general reduction of tropical surface wind speed (-0.15 m s^{-1}/-2.6%; RCP8.5) discussed by Held and Soden (2006). Both these reductions are, however, moderately correlated ($r = 0.48$, $p = 0.95$) across the models. This may be due to a common underlying mechanism (Bayr & Dommenget, 2013), in which the lower tropospheric humidity constrains the amplitude of the tropospheric warming and SLP change and hence that of the circulation change.

The expected decrease of the ISM circulation depicted in CMIP models can already be detected in observations over the last half-century (Fan et al., 2010). In contrast, there is no consistent trend in the observed winds over the AS region in winter (Figure S8e). The decreasing trend detected by CMIP models is, however, entirely within the range of the model's internal variability until the year 2030 (Figures S8a and S8c for RCP8.5 and Figures S8b and S8d for 4.5), which explains why such a trend is not yet detectable in observations. The projected AS wind speed by 2100 is 2.2 ± 0.3 (1.2 ± 0.2) times larger than the present-day internal nonseasonal, and hence interannual, variability in RCP8.5 (RCP4.5).

The increased winter rainfall over the equatorial IO has implications for regional water resources. The projected rainfall increase is significant mostly over the ocean but may be socioeconomically relevant for the east African countries and the islands located in the equatorial IO. In contrast, the rainfall change over southern India and Sri Lanka is not statistically significant. The projected changes in regional rainfall are, however, highly sensitive to CMIP model biases (e.g., Hwang & Frierson, 2013; Sabeerali et al., 2015) and hence need further assessment.

These IWM circulation changes are potentially important for the AS biogeochemistry. Previous studies have mainly focused on summer AS productivity, with some of them suggesting a decline due to increased thermal stratification (Roxy et al., 2016) while the others suggesting an increase due to a poleward shift of the monsoon jet (Praveen et al., 2016). The northern AS winter bloom contributes significantly to the annual AS productivity, but its response to climate change has so far not been discussed. This bloom is largely the result of the convective entrainment of nutrients into the mixed layer during winter (e.g., Keerthi et al., 2017; Prasanna Kumar et al., 2001). The projected weakening of the winter AS winds will reduce the oceanic stirring (Figure S5) and heat losses (Figures 3a and 3c) to the atmosphere over the northern part of the basin. This will in turn reduce the winter mixed layer deepening (Figures 3b and 3d) and hence the amount of nutrients entraining into the mixed layer, leading to a possible reduction in the AS productivity during winter. The winter convective overturning not only influences the AS productivity but also ventilates the upper boundary of the AS oxygen minimum zone (Morrison et al., 1999), which is one of the most intense in the world oceans. The reduced winter ventilation may further contribute to the projected expansion of the AS oxygen minimum zone in the future (Bopp et al., 2013). These issues will be addressed in a future study.

Acknowledgments
We thank the Director, CSIR-NIO, for his support. This work was done while M. L. and T. I. were visiting scientists at the CSIR-National Institute of Oceanography (CSIR-NIO) under Institut de Recherche pour le Développement (IRD) funding. J. V. acknowledges IRD for supporting regular visits to CSIR-NIO and thanks CSIR-NIO for his "Adjunct Scientist" position. I. S. acknowledges financial support from CSIR, New Delhi, and INCOIS/MoES (HOOFS project). P. V. is funded through a CSIR Senior Research Fellow grant and thanks Hema Naik for her support. We acknowledge the World Climate Research Program's Working Group on Coupled Modelling, which is responsible for CMIP, and we thank the climate modeling groups (listed in Table S1) for producing and making available their model outputs. All the CMIP5 model outputs were downloaded from the Institut Pierre Simon Laplace (IPSL) CICLAD repository. This is NIO contribution 6102.

References

Banse, K., & McClain, C. R. (1986). Winter blooms of phytoplankton in the Arabian Sea as observed by the coastal zone colour scanner. *Marine Ecology Progress Series*, *34*, 201–211.

Bayr, T., & Dommenget, D. (2013). The tropospheric land-sea warming contrast as the driver of tropical sea level pressure changes. *Journal of Climate*, *26*, 1387–1402.

Boer, G. J. (2011). The ratio of land to ocean temperature change under global warming. *Climate Dynamics*, *37*(11–12), 2253–2270.

Bopp, L., Resplandy, L., Orr, J. C., Doney, S. C., Dunne, J. P., Gehlen, M., … Vichi, M. (2013). Multiple stressors of ocean ecosystems in the 21st century: Projections with CMIP5 models. *Biogeosciences*, *10*, 6225–6245.

Bracegirdle, T. J., & Stephenson, D. B. (2012). Higher precision estimates of regional polar warming by ensemble regression of climate model projections. *Climate Dynamics*, *39*, 2805–2821.

Bracegirdle, T. J., & Stephenson, D. B. (2013). On the robustness of emergent constraints used in multimodel climate change projections of Arctic warming. *Journal of Climate*, *26*, 669–678.

Christensen, J. H., Krishna Kumar, K., Aldrian, E., An, S.-I., Cavalcanti, I. F. A., de Castro, M., … Zhou, T. (2013). Climate phenomena and their relevance for future regional climate change. In T. F. Stocker, et al. (Eds.), *Climate Change 2013: The Physical Science Basis. Contribution of Working Group I to the Fifth Assessment Report of the Intergovernmental Panel on Climate Change* (pp. 1217–1308). Cambridge, UK, and New York: Cambridge University Press.

Cox, P. M., Pearson, D., Booth, B. B., Friedlingstein, P., Huntingford, C., Jones, C. D., & Luke, C. M. (2013). Sensitivity of tropical carbon to climate change constrained by carbon dioxide variability. *Nature*, *494*(7437), 341–344.

de Boyer Montégut, C., Madec, G., Fischer, A. S., Lazar, A., & Iudicone, D. (2004). Mixed layer depth over the global ocean: An examination of profile data and a profile-based climatology. *Journal of Geophysical Research*, *109*, C12003. https://doi.org/10.1029/2004JC002378

Dee, D. P., Uppala, S. M., Simmons, A. J., Berrisford, P., Poli, P., Kobayashi, S., … Vitart, F. (2011). The ERA-Interim reanalysis: Configuration and performance of the data assimilation system. *Quarterly Journal of the Royal Meteorological Society*, *137*, 553–597.

Dimri, A. P., Niyogi, D., Barros, A. P., Ridley, J., Mohanty, U. C., Yasunari, T., & Sikka, D. R. (2015). Western disturbances: A review. *Reviews of Geophysics*, *53*, 225–246. https://doi.org/10.1002/2014RG000460

Dommenget, D. (2009). The ocean's role in continental climate variability and change. *Journal of Climate*, *22*, 4939–4952.

Endo, H., & Kitoh, A. (2016). Projecting Changes of the Asian Summer Monsoon through the Twenty-First Century. In L. M. V. Carvalho & C. Jones (Eds.), *The Monsoons and Climate Change: Observations and Modeling* (pp. 47–66). Springer.

Fan, F., Mann, M. E., Lee, S., & Evans, J. L. (2010). Observed and modeled changes in the South Asian summer monsoon over the historical period. *Journal of Climate*, *23*, 5193–5205.

Findlater, J. (1971). *Mean Monthly Airflow at Low Levels Over the Western Indian Ocean*, *Geophysical Memoirs*, (No. 115, pp. 53). London: HMSO.

Gadgil, S. (2003). The Indian monsoon and its variability. *Annual Review of Earth and Planetary Sciences*, *31*(1), 429–467.

Gadgil, S., & Gadgil, S. (2006). The Indian monsoon, GDP and agriculture. *Economic and Political Weekly*, *41*, 4887–4895.

Gill, A. E. (1982). *Atmosphere-Ocean Dynamics* (662 pp.). San Diego, CA: Academic.

Goswami, B. N., Venugopal, V., Sengupta, D., Madhusoodanan, M., & Xavier, P. K. (2006). Increasing trend of extreme rain events over India in a warming environment. *Science*, *314*, 1442–1445.

Held, I. M., & Soden, B. J. (2006). Robust responses of the hydrological cycle to global warming. *Journal of Climate*, *19*, 5686–5699.

Hwang, Y.-T., & Frierson, D. M. W. (2013). Link between the double-Intertropical Convergence Zone problem and cloud bias over Southern Ocean. *Proceedings of the National Academy of Sciences of the United States of America*, *110*, 4935–4940. https://doi.org/10.1073/pnas.1213302110

Jiang, D., & Tian, Z. (2013). East Asian monsoon change for the 21st century: Results of CMIP3 and CMIP5 models. *Chinese Science Bulletin*, *58*(12), 1427–1435.

Joshi, M. M., Gregory, J. M., Webb, M. J., Sexton, D. M. H., & Johns, T. C. (2008). Mechanisms for the land/sea warming contrast exhibited by simulations of climate change. *Climate Dynamics*, *30*(5), 455–465.

Keerthi, M. G., Lengaigne, M., Levy, M., Vialard, J., Parvathi, V., de Boyer Montegut, C., … Muraleedharan, P. M. (2017). Physical control of interannual variations of the winter chlorophyll bloom in the northern Arabian Sea. *Biogeosciences*, *14*, 3615–3632. https://doi.org/10.5194/bg-14-3615-2017

Kitoh, A. (2017). The Asian monsoon and its future change in climate models: A review. *Journal of the Meteorological Society of Japan. Series II*, *95*(1), 7–33.

Levine, R. C., Turner, A. G., Marathayil, D., & Martin, G. M. (2013). The role of northern Arabian Sea surface temperature biases in CMIP5 model simulations and future projections of Indian summer monsoon rainfall. *Climate Dynamics*, *41*(1), 155–172.

Li, G., Xie, S.-P., & Du, Y. (2016). A robust but spurious pattern of climate change in model projections over the tropical Indian Ocean. *Journal of Climate*, *29*, 5589–5608.

Li, G., Xie, S.-P., Du, Y., & Luo, Y. (2016). Effects of excessive equatorial cold tongue bias on the projections of tropical Pacific climate change. Part I: The warming pattern in CMIP5 multi-model ensemble. *Climate Dynamics*, *47*, 3817–3831.

Madhupratap, M., Nair, K. N. V., Gopalkrishnan, T. C., Haridas, P., Nair, K. K. C., & Venugopal, P. (2001). Arabian Sea oceanography and fisheries of the west coast of India. *Current Science*, *81*, 355–361.

Madhupratap, M., Prasanna Kumar, S., Bhattathiri, P. M. A., Kumar, M. D., Raghukumar, S., Nair, K. K. C., & Ramaiah, N. (1996). Mechanism of the biological response to winter cooling in the northeastern Arabian Sea. *Nature*, *384*, 549–552.

Marathayil, D., A. G. Turner, L. C. Shaffrey, and R. C. Levine (2013), Systematic winter sea-surface temperature biases in the northern Arabian Sea in HiGEM and the CMIP3 models, *Environmental Research Letters 8*(1), 014028.

Marra, J., & Barber, R. T. (2005). Primary productivity in the Arabian Sea: A synthesis of JGOFS data. *Progress in Oceanography*, *65*(2), 159–175.

Morrison, J. M., Codispoti, L. A., Smith, S. L., Wishner, K., Flagg, C., Gardner, W. D., … Gundersen, J. S. (1999). The oxygen minimum zone in the Arabian Sea during 1995. *Deep Sea Research, Part II*, *46*, 1903–1931.

Moss, R. H., Edmonds, J. A., Hibbard, K. A., Manning, M. R., Rose, S. K., van Vuuren, D. P., … Wilbanks, T. J. (2010). The next generation of scenarios for climate change research and assessment. *Nature*, *463*, 747–756.

Ogata, T., Ueda, H., Inoue, T., Hayasaki, M., Yoshida, A., Watanabe, S., … Kumai, A. (2014). Projected future changes of the Asian Monsoon: A comparison of CMIP3 and CMIP5 model results. *Journal of the Meteorological Society of Japan*, *92*, 207–225.

Prasanna Kumar, S., Ramaiah, N., Gauns, M., Sarma, V. V. S. S., Muraleedharan, P. M., Raghukumar, S., … Madhupratap, M. (2001). Physical forcing of biological productivity in the northern Arabian Sea during the northeast monsoon. *Deep Sea Research Part II: Topical Studies in Oceanography*, *48*(6–7), 1115–1126.

Praveen Kumar, B., Vialard, J., Lengaigne, M., Murty, V. S. N., & McPhaden, M. (2012). TropFlux: Air-sea fluxes for the global tropical oceans: Description and evaluation. *Climate Dynamics*, *38*(7–8), 1521–1543.

Praveen, V., Ajayamohan, R. S., Valsala, V., & Sandeep, S. (2016). Intensification of upwelling along Oman coast in a warming scenario. *Geophysical Research Letters*, *43*, 7581–7589. https://doi.org/10.1002/2016GL069638

Rajeevan, M., Unnikrishnan, C. K., Bhate, J., Niranjan Kumar, K., & Sreekala, P. P. (2012). Northeast monsoon over India: Variability and prediction. *Meteorological Applications*, *19*, 226–236.

Roxy, M. K., Ritika, K., Terray, P., Murtugudde, R., Ashok, K., & Goswami, B. N. (2015). Drying of Indian subcontinent by rapid Indian Ocean warming and a weakening land-sea thermal gradient. *Nature Communications*, *6*, 7423.

Roxy, M. K., Modi, A., Murtugudde, R., Valsala, V., Panickal, S., Prasanna Kumar, S., … Levy, M. (2016). A reduction in marine primary productivity driven by rapid warming over the tropical Indian Ocean. *Geophysical Research Letters*, *43*, 826–833.

Sabeerali, C. T., Rao, S. A., Dhakate, A. R., Salunke, K., & Goswami, B. N. (2015). Why ensemble mean projection of south Asian monsoon rainfall by CMIP5 models is not reliable? *Climate Dynamics*, *45*(1–2), 161–174.

Saji, N. H., Goswami, B. N., Vinayachandran, P. N., & Yamagata, T. (1999). A dipole mode in the tropical Indian Ocean. *Nature*, *401*, 360–363.

Sandeep, S., & Ajayamohan, R. S. (2014). Origin of cold bias over the Arabian Sea in climate model. *Scientific Reports*, *4*, 6403.

Sandeep, S., & Ajayamohan, R. S. (2015). Poleward shift in Indian summer monsoon low level jetstream under global warming. *Climate Dynamics*, *45*, 337–351.

Sharmila, S., Joseph, S., Sahai, A. K., Abhilash, S., & Chattopadhyay, R. (2015). Future projection of Indian summer monsoon variability under climate changes cenario: An assessment from CMIP5 climate models. *Global and Planetary Change*, *124*, 62–78.

Siew, J. H., Tangang, F. T., & Juneng, L. (2014). Evaluation of CMIP5 coupled atmosphere-ocean general circulation models and projection of the Southeast Asian winter monsoon in the 21st century. *International Journal of Climatology*, *34*, 2872–2884.

Smith, S. L., & Madhupratap, M. (2005). Mesozooplankton of the Arabian Sea: Patterns influenced by seasons, upwelling, and oxygen concentrations. *Progress in Oceanography*, *65*, 214–239.

Sobel, A. H., Nilsson, J., & Polvani, L. M. (2001). The weak temperature gradient approximation and balanced tropical moisture waves. *Journal of the Atmospheric Sciences*, *58*, 3650–3665.

Sooraj, K. P., Terray, P., & Mujumdar, M. (2015). Global warming and the weakening of the Asian summer Monsoon circulation: Assessments from the CMIP5 models. *Climate Dynamics*, *45*, 1–20.

Sperber, K. R., Annamalai, H., Kang, I. S., Kitoh, A., Moise, A., Turner, A., … Zhou, T. (2013). The Asian summer monsoon: An intercomparison of CMIP5 vs. CMIP3 simulations of the late 20th century. *Climate Dynamics*, *41*(9–10), 2711–2744.

Trenberth, K. E., Stepaniak, D. P., & Caron, J. M. (2000). The global monsoon as seen through the divergent atmospheric circulation. *Journal of Climate*, *13*(22), 3969–3993.

Turner, A. G., & Annamalai, H. (2012). Climate change and the South Asian summer monsoon. *Nature Climate Change*, *2*, 587–595.

Vialard, J., Terray, P., Duvel, J. P., Nanjundiah, R. S., Shenoi, S. S. C., & Shankar, D. (2011). Factors controlling January–April rainfall over southern India and Sri Lanka. *Climate Dynamics*, *37*(3–4), 493–507.

Webster, P. J., Magana, V. O., Palmer, T. N., Tomas, T. A., Yanai, M., & Yasunari, T. (1998). Monsoons: Processes, predictability, and prospects for prediction. *Journal of Geophysical Research: Oceans*, *103*, 14,451–14,510. https://doi.org/10.1029/97JC02719